

## Supporting Information

### **Prefabricated covalent organic framework with double vacancies: anchoring Cu for highly efficient photocatalytic H<sub>2</sub> evolution**

Ying Zang,<sup>a</sup> Rui Wang,<sup>a</sup> Peng-Peng Shao,<sup>b</sup> Xiao Feng,<sup>b</sup> Shan Wang<sup>\*a</sup>, Shuang-Quan Zang<sup>\*a</sup> and Thomas C. W. Mak<sup>a, c</sup>

a. Green Catalysis Center, and College of Chemistry, Zhengzhou University Zhengzhou 450001 (China)

b. Beijing Key Laboratory of Photoelectronic/Electrophotonic Conversion Materials, Key Laboratory of Cluster Science, Ministry of Education, School of Chemistry and Chemical Engineering, Beijing Institute of Technology Beijing 100081, P. R. China

c. Department of Chemistry, The Chinese University of Hong Kong Shatin, New Territories, Hong Kong SAR, China

[zangsqzg@zzu.edu.cn](mailto:zangsqzg@zzu.edu.cn) ; [shanwang@zzu.edu.cn](mailto:shanwang@zzu.edu.cn)

## Materials and Methods

**Materials and reagents.** All chemicals were purchased through commercial suppliers and used without further purification. Water used in this work was purified using the Milli-Q purification system. Copper(II) acetate monohydrate, and triethylamine were purchased from Sinopharm Chemical Reagent Co., Ltd., China. Furthermore, 2,3,6,7,10,11-hexaaminotriphenylene hexahydrochloride (HATP·6HCl) was prepared according to the procedure available in the literature.<sup>1,2</sup>

### Synthesis of Salphen-HDCOF

Triethylamine (Et<sub>3</sub>N) (25%, 1 mL) was added in a suspension of HATP·6HCl (50 mg, 0.095 mmol) in MeOH at 80 °C in Ar, the mixture was stirred for 20 min, then the solution of DFP (145mg 0.95mmol) was added. The reaction was going on 24 h. After cooling to room temperature, the precipitate was collected by filtration, and washed with N,N-Dimethylformamide (3 × 5 mL), acetone (2 × 5 mL) and tetrahydrofuran (2 × 5 mL). The solid was dried in a vacuum oven at 60 °C to afford Salphen-HDCOF as a dark brown powder. Anal. Calcd. for (C<sub>204</sub>H<sub>84</sub>N<sub>30</sub>O<sub>12</sub>)<sub>n</sub>: (EA calcd. (%) for C<sub>204</sub>H<sub>84</sub>N<sub>30</sub>O<sub>12</sub>: C, 77.86; N, 13.35; H, 2.69; found: C 76.51, H 1.85, N 12.63).

### Synthesis of Synthesis of Cu-Salphen-HDCOF

Salphen-HDCOF (50 mg) was added in the solution of Cu(OAc)<sub>2</sub>·H<sub>2</sub>O (200 mg) in MeOH (100 mL) at room temperature, then the mixture was stirred for 3 days. The precipitate in dark brown was collected after centrifuged, washed with MeOH for 12 h to ensure complete removal of residual Cu(OAc)<sub>2</sub>, and then dried under vacuum, to give Cu-Salphen-HDCOF (C<sub>204</sub>H<sub>72</sub>N<sub>30</sub>O<sub>12</sub>Cu<sub>12</sub>)<sub>n</sub>. (EA calcd. (%) for C<sub>204</sub>H<sub>72</sub>N<sub>30</sub>O<sub>12</sub>Cu<sub>12</sub>: C 62.87, H 1.86, N 11.8, Cu 19.6; found: C 63.14, H 2.76, N 12.63, Cu 15.63).

### Synthesis of Salphen-HDCOF-NSs

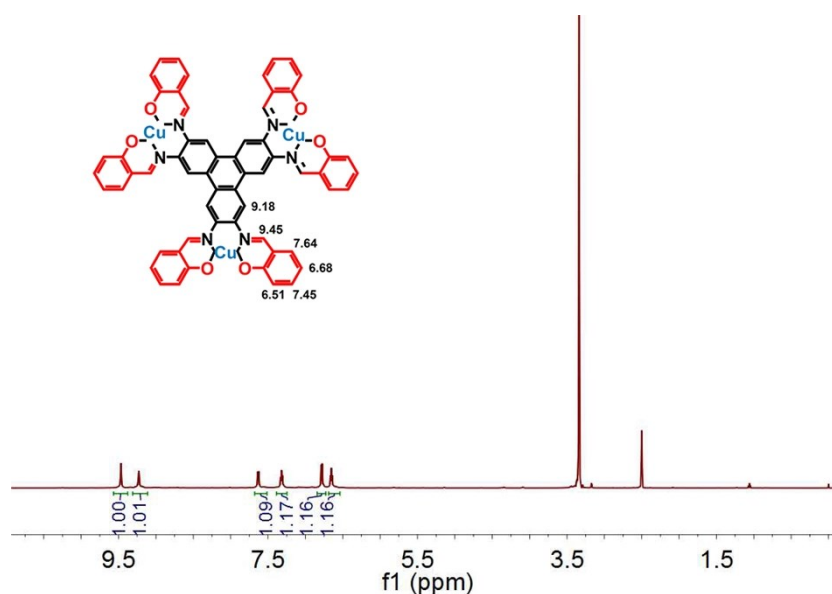
Salphen-HDCOF (5 mg) was added in MeOH (20 mL), the mixture was ultrasound for 24 h, then stand the solution for 3 days, until the supernatant is colorless and clear and shows Tyndall effect. The Salphen-HDCOF-NSs was obtained.

### Synthesis of Cu-Salphen-HDCOF-NSs

Cu-Salphen-HDCOF (5 mg) was added in MeOH (20 mL), the mixture was ultrasound for 24 hours, then stand the solution for 3 days, until the supernatant is colorless and clear and shows Tyndall effect. The Cu-Salphen-HDCOF-NSs was obtained.

### Synthesis of TSCu<sub>3</sub>

A MeOH solution (1.0 mL) of Cu(II) acetate dihydrate (0.018 g, 0.08 mmol) was added to the suspension of HATP·6HCl (12.8 mg, 0.014mmol) in MeOH (6.0 mL) was added, and the mixture was stirred at room temperature for 3 days. A red-orange precipitate was collected by filtration, washed with MeOH (5.0 × 3 mL), and dried under vacuum, to give a TSCu<sub>3</sub>.<sup>62</sup> <sup>1</sup>H NMR (DMSO-d<sub>6</sub>) δ (ppm) 9.45 (s, 6H, CH=N), 9.18 (s, 6H, triphenylene CH), 7.64 (d, J = 7.1 Hz, 6H, aromatic CH), 7.45 (t, J = 7.2 Hz, 6H, aromatic CH), 6.68 (d, J = 8.4 Hz, 6H, aromatic CH), 6.51 (t, J = 7.2 Hz, 6H, aromatic CH). MALDI-TOF MS for C<sub>60</sub>H<sub>36</sub>N<sub>6</sub>O<sub>6</sub>Cu<sub>3</sub> (Calcd. 1127.62), m/z = 1126.16 ([M]<sup>+</sup>, 100%).



### Material characterization

The PXRD patterns were recorded on a Rigaku MiniFlex 600 diffractometer at 30 kV, and Cu-K $\alpha$  ( $\lambda = 1.5418 \text{ \AA}$ ) at ambient temperature.

The X-ray photoelectron spectroscopy (XPS) measurements were tested using ESCALAB 250 system (Thermo Electron) with an Al K $\alpha$  (300 W) X-ray resource (3.82 eV versus absolute vacuum value).

Fourier transform infrared (FT-IR) spectra were recorded on a Bruker ALPHA II FT-IR spectrometer.

Solid state UV-vis absorption spectra were measured on a UH4150 UV-Vis/NIR spectrophotometer.

<sup>13</sup>C MAS solid-state NMR experiments were performed on Agilent 600 DD2 spectrometer at a resonance frequency of 150.15 MHz. <sup>13</sup>C NMR spectra were recorded with spinning rate of 15k Hz with a 4mm probe at room temperature. <sup>13</sup>C CPMAS experiments were performed with a delay time of 5s. Scan number: 2048 scans.

<sup>1</sup>H NMR spectra were recorded on a Bruker DRX spectrometer operating at 400 MHz in DMSO.

Element analyses (EA) were measured on Thermo Flash EA 1112.

Inductively coupled plasma mass spectrometry (ICP-MS) were recorded with OptiMass 9500/NMR-213.

Nitrogen sorption isotherms were measured in 77 K nitrogen by using automatic volumetric adsorption equipment (Belsorp Max) after a degassed process at 80°C for 12 h. Specific surface areas were obtained by using the Brunauer-Emmet-Teller (BET) model, pore size distributions were simulated by the nonlocal density functional theory (NLDFT) model.

Field-emission scanning electron microscopy (FESEM) measurement was carried out using Zeiss Sigma 500.

The transmission electron microscopy (TEM) and high-resolution transmission electron microscopy (HRTEM) images were obtained in JEM-2100 equipment.

Atomic Force Microscope (AFM) was recorded with AIST-NT SmartSPM.

Photoluminescence spectra were determined by a Horiba Scientific FluoroMax-4 spectrofluorometer spectrometer.

Luminescence decay was measured on a HORIBA FluoroLog-3 fluorescence spectrometer equipped with a 355 nm laser operating in time-correlated single-photon counting mode (TCSPC) with a resolution time of 340  $\mu$ s.

Transient photocurrent/time curves of the bare glassy carbon electrode, electrode coated by FS and Cu-Salphen-HDCOF, TSCu<sub>3</sub> or Salphen-HDCOF with Nafion in a PBS electrolyte (pH=7.2~7.4) at a bias of 0.0 V and on the condition of light on and light off. Conditions: glassy carbon as working electrode, Pt plate as counter electrode, and Ag/AgCl as reference electrode. Working electrode preparation: the object samples were dispersed in water by ultrasonication for 20 minutes, dripped on glassy carbon (GC) electrode ( $S = 0.071 \text{ cm}^2$ ), and then dried in the air.

### **Structure simulations**

Molecular modeling and Pawley refinement were carried out using Materials Studio 2017R2 (Accelrys). The pronounced PXRD patterns illustrate their high crystallinity. Indexing the experimental PXRD indicates the formation of a hexagonal lattice. According to the planarity and symmetry of the monomers, we anticipated a stacking of two-dimensional (2D) trigonal layers, and constructed eclipsed bnn ( $P6$ ) and staggered gra ( $P3$ ) modes with trigonal and linear building blocks positioned on the corresponding nodes. The cell parameters were obtained through Pawley refinement of the experimental data iteratively until the Rwp and Rp value converges. Force-field calculations using the universal force field (UFF) using charges Qeq were employed to optimize the bond length and angles subject to the minimization of the structural energy.

### **XAFS measurements**

The X-ray absorption fine structure spectra (Cu K-edge) were collected at 1W1B beamline of Beijing Synchrotron Radiation Facility (BSRF). The data were collected in transmission mode using a Lytle detector. The samples were grinded and uniformly daubed on the special adhesive tape. The energy range of 4B9A and 1W2A beam line is 5k ev-20k ev. The energy range of monochromator is better than  $3 \times 10^3$  in this line. The intensity range of Beam line is  $2 \times 10^9$ - $2 \times 10^{10}$  cps. The spot size at the sample is  $0.8 \times 0.9$  mm<sup>2</sup>.

### **General procedures for photocatalytic hydrogen evolution**

Photocatalytic reaction was conducted in a 60 mL Pyrex cell with white LED (light intensity, 80 mW/cm<sup>2</sup>,  $\lambda > 420$  nm) as a light source. In a typical photocatalytic experiment, the catalyst (0.5 mg) was suspended in H<sub>2</sub>O/MeOH (v:v = 1:1) containing TEA (2 mL) and FS (5.0 mg). Before irradiation, the suspension of the catalyst was dispersed in an ultrasonic bath for 30 minutes, and then N<sub>2</sub> was bubbled through the reaction mixture for 20 minutes to completely remove oxygen. The whole process was done under atmosphere pressure. The amount of produced H<sub>2</sub> was monitored in real time by GC analysis of the headspace gases by using an Agilent GC7820 Gas Chromatograph (N<sub>2</sub> as gas carrier).

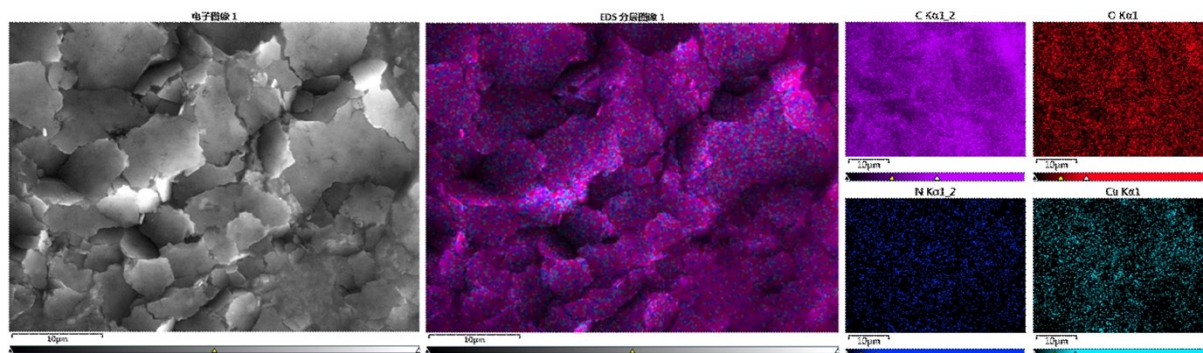


Figure S1. SEM image and energy dispersive spectroscopy (EDS) mapping results of the Cu-Salphen-HDCOF, showing uniform distribution of C, O, N and Cu.

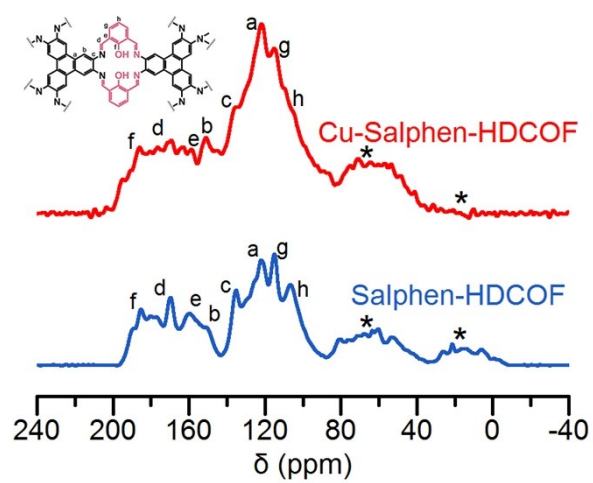


Figure S2. Solid-state CP-MAS  $^{13}\text{C}$ -NMR spectra of Salphen-HDCOF and Cu-Salphen-HDCOF.

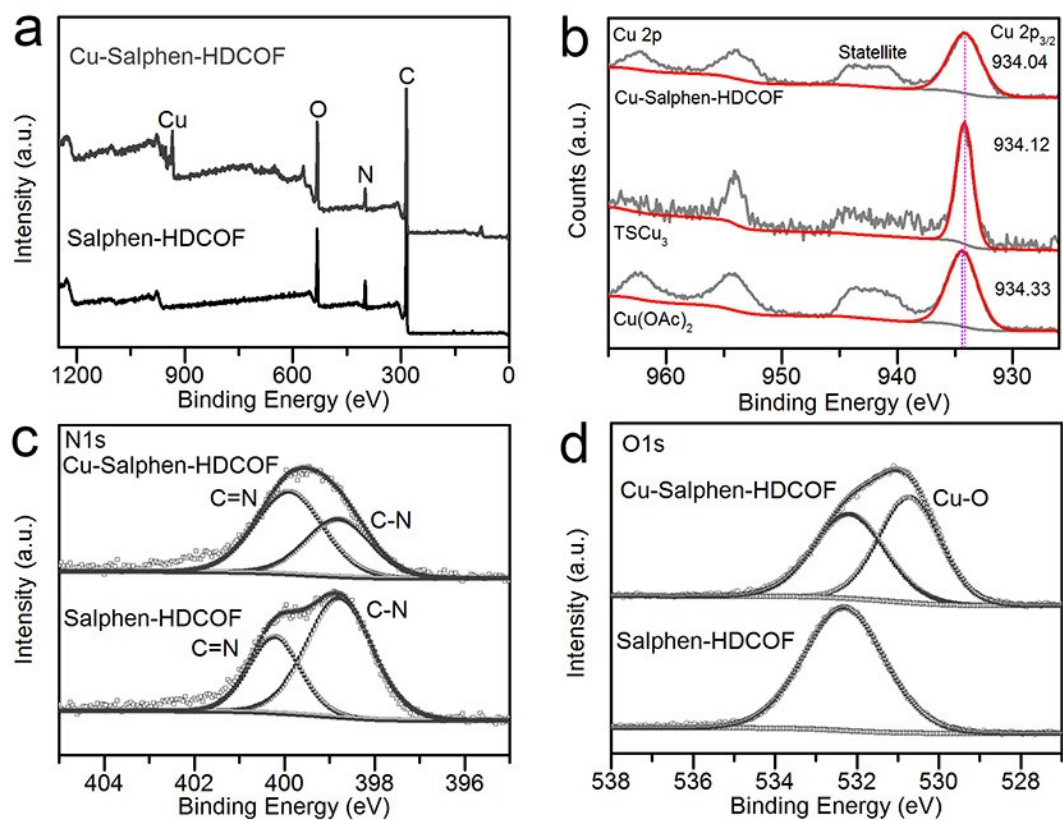


Figure S3. XPS analysis (a) Energy survey spectrum of Salphen-HDCOF and Cu-Salphen-HDCOF. High-resolution spectrum in the (b) Cu2p region of Cu-Salphen-HDCOF, TSCu<sub>3</sub> and Cu(OAc)<sub>2</sub>, (c) N1s region and (d) O1s region, respectively.

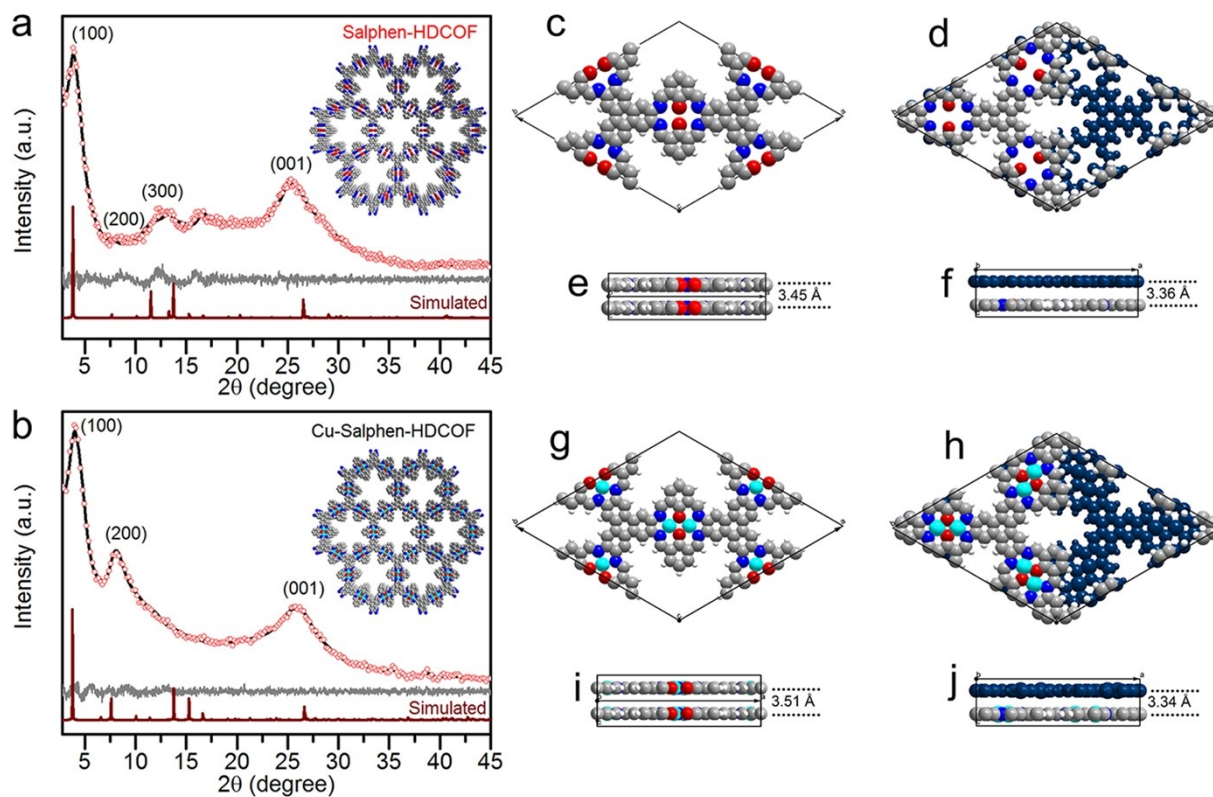


Figure S4. To elucidate their crystal structures, structural models with eclipsed AA stacking and staggered AB stacking were constructed using Materials Studio software. PXRD patterns of Salphen-HDCOF (a) and Cu-Salphen-HDCOF (b) with the experimental profiles in red pot, Pawley-refined profiles in black line, calculated profiles in wine line (AA stacking), and the differences between the experimental and refined PXRD patterns in gray line. Unit cell of Salphen-HDCOF with AA stacking (c) and AB stacking (d), Crystal structure of layers in Salphen-HDCOF with AA stacking (e) and AB stacking (f), the interlayer distance is 3.45 Å with AA stacking and 3.36 Å with AB stacking. Unit cell of Salphen-HDCOF with AA stacking (g) and AB stacking (h), Crystal structure of layers in Cu-Salphen-HDCOF with AA stacking (i) and AB stacking (g), the interlayer distance is 3.51 Å with AA stacking and 3.34 Å with AB stacking.

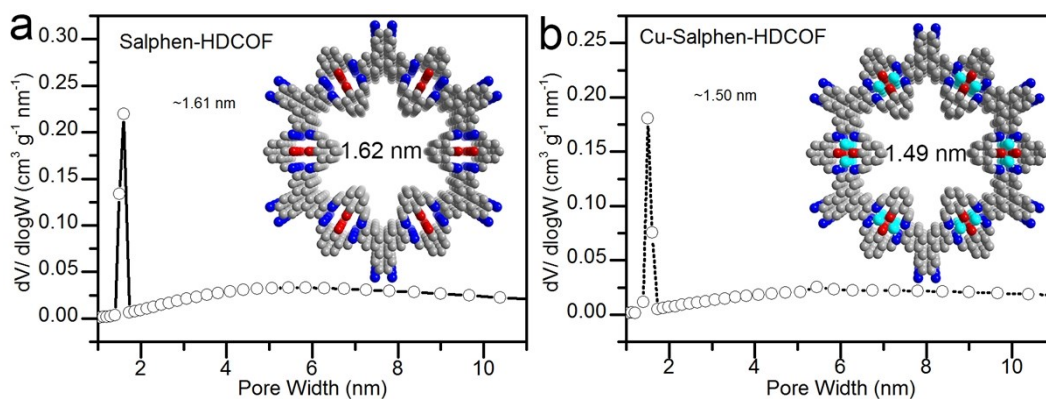


Figure S5. Pore size distributions calculated by non-local density functional theory (NLDFT) exhibited pore diameters of 1.61 nm for Salphen-HDCOF (a) and 1.50 nm for Cu-Salphen-HDCOF (b), respectively, which are in good agreement with predicted hexagonal pores.

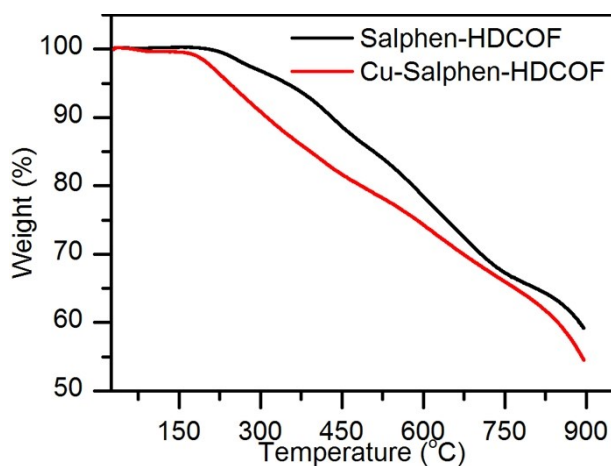


Figure S6. Thermogravimetric analysis (TGA) curves of Salphen-HDCOF and Cu-Salphen-HDCOF.

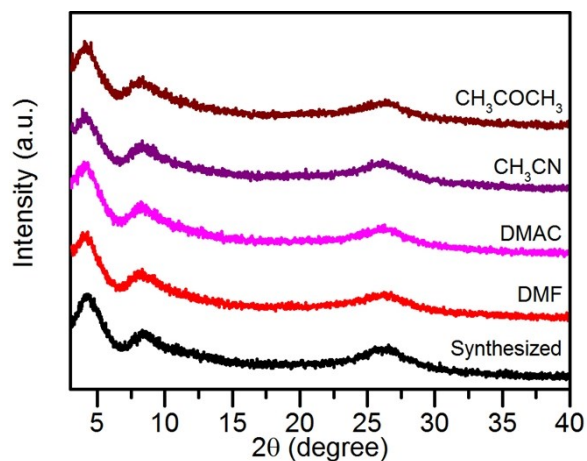


Figure S7. PXRD patterns of Cu-Salphen-HDCOF after soaking in various organic solvents for 36 h.

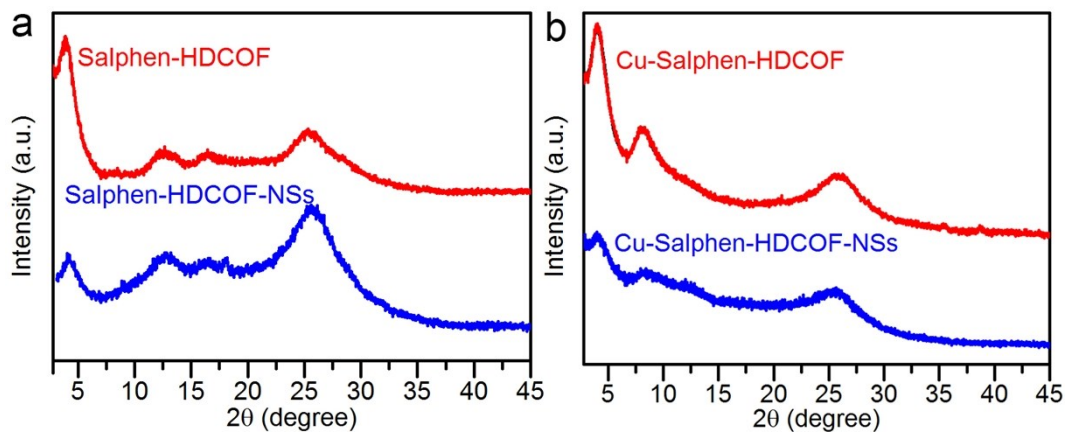


Figure S8. PXRD patterns of Salphen-HDCOF-NSs (a) and Cu-Salphen-HDCOF-NSs (b).

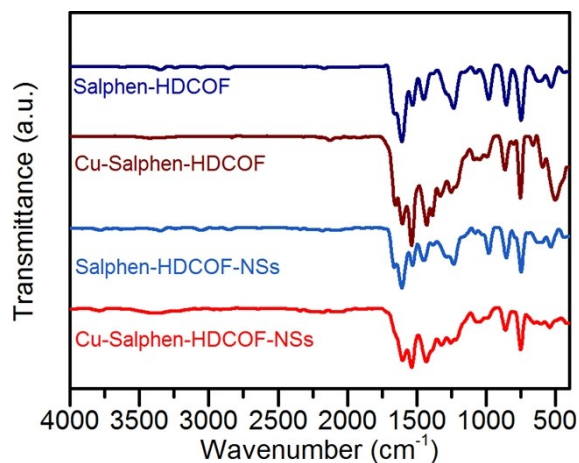


Figure S9. FT-IR spectra of Salphen-HDCOF-NSs and Cu-Salphen-HDCOF-NSs, which revealed that the exfoliated nanosheets preserved their structural integrity.

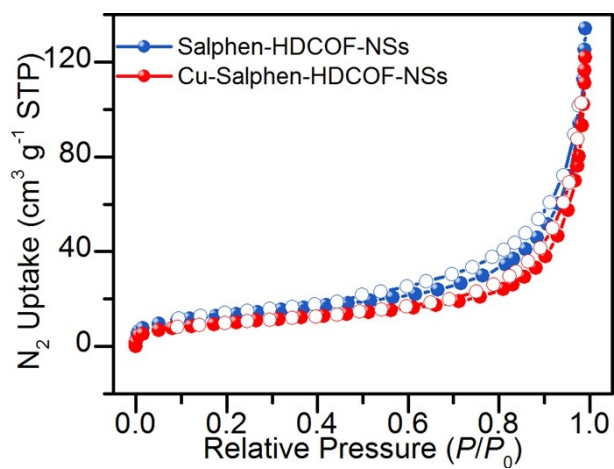


Figure S10. N<sub>2</sub> adsorption-desorption isotherms of Salphen-HDCOF-NSs and Cu-Salphen-HDCOF-NSs.

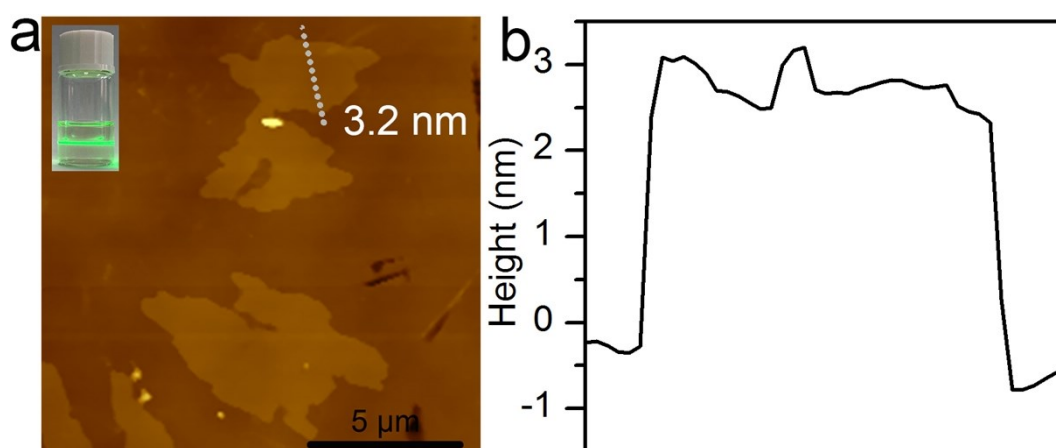


Figure S11. (a) AFM images of Salphen-HDCOF-NSs. Inset of (a) is the Tyndall effect of Salphen-HDCOF-NSs in  $\text{CH}_3\text{OH}$ ; (b) Height plot of Salphen-HDCOF-NSs.

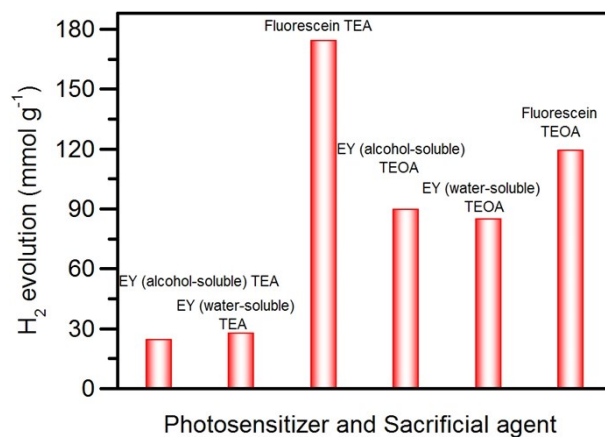


Figure S12. The effect of photosensitizer and sacrificial agent on H<sub>2</sub> evolution. H<sub>2</sub> evolution condition: MeOH/H<sub>2</sub>O (1:1) in the presence of 2 mg of Cu-Salphen-HDCOF-NSs in 30 mL solution containing sacrificial agent (2 mL) and 10 mg of photosensitizer under an inert atmosphere. The system was irradiated with a visible-light.

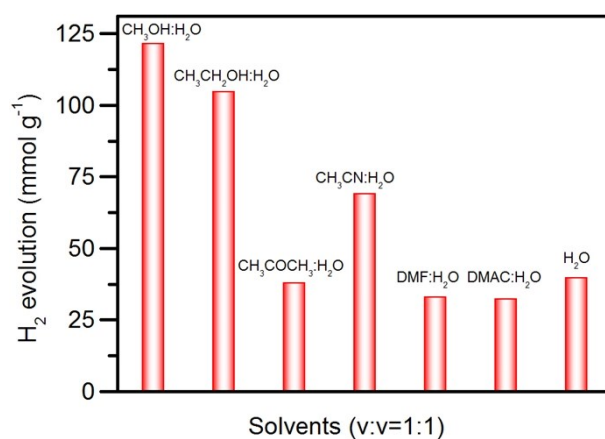


Figure S13. The effect of solvents on H<sub>2</sub> evolution. H<sub>2</sub> evolution condition: 2 mg of Cu-Salphen-HDCOF-NSs in 30 mL solution containing TEA (2 mL) and 10 mg of FS (Fluorescence) under an inert atmosphere. The system was irradiated with a visible-light.

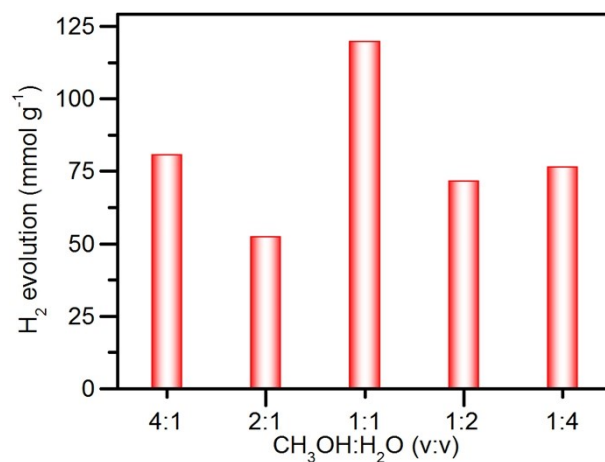


Figure S14. The effect of the solvents ratio on H<sub>2</sub> evolution. H<sub>2</sub> evolution condition: 2 mg of Cu-Salphen-HDCOF-NSs in 30 mL solution containing TEA (2 mL) and 10 mg of FS (Fluorescence) under an inert atmosphere. The system was irradiated with a visible-light.

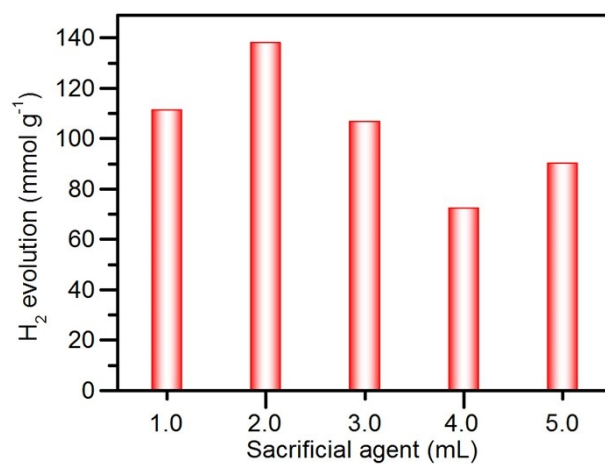


Figure S15. The effect of the volume of sacrificial agent on H<sub>2</sub> evolution. H<sub>2</sub> evolution condition: MeOH/H<sub>2</sub>O (1:1) in the presence of 2 mg of Cu-Salphen-HDCOF-NSs and 10 mg of FS (Fluorescence) under an inert atmosphere. The system was irradiated with a visible-light.

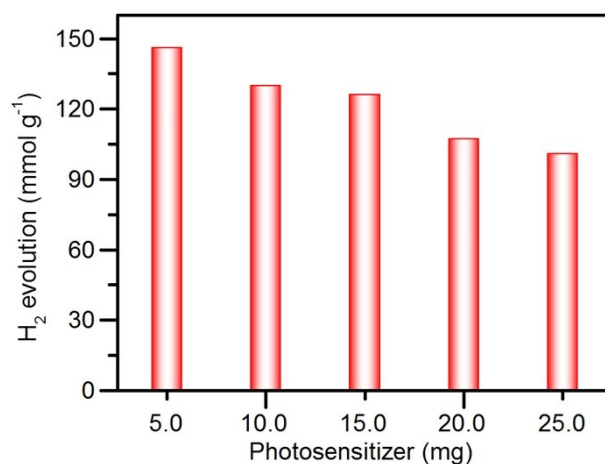


Figure S16. The effect of the different mass of photosensitizer on H<sub>2</sub> evolution. H<sub>2</sub> evolution condition: MeOH/H<sub>2</sub>O (1:1) in the presence of 2 mg of Cu-Salphen-HDCOF-NSs in 30 mL solution containing TEA (2 mL) under an inert atmosphere. The system was irradiated with a visible-light.

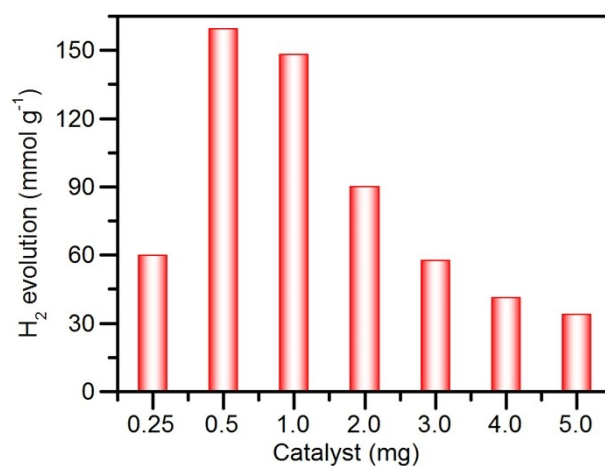


Figure S17. The effect of the different mass of catalyst on H<sub>2</sub> evolution. H<sub>2</sub> evolution condition: MeOH/H<sub>2</sub>O (1:1) in the presence of 5 mg of FS (Fluorescence) in 30 mL solution containing TEA (2 mL) under an inert atmosphere. The system was irradiated with a visible-light.

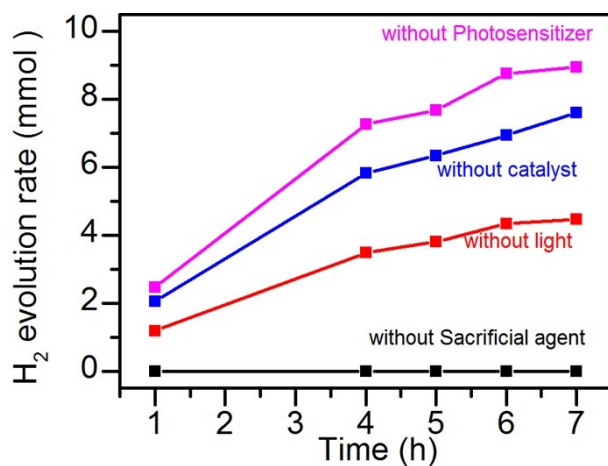


Figure S18. Control experiments in the absence of photosensitizer, Cu-Salphen-HDCOF-NSs, light or sacrificial agent of catalytic systems.

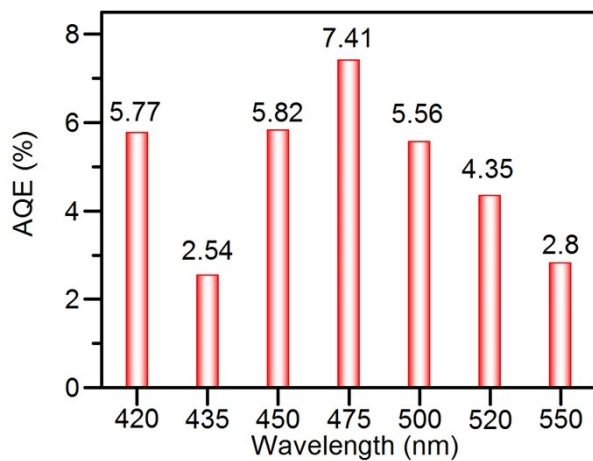


Figure S19. The apparent quantum efficiency (AQE) of catalytic system under irradiation with monochromatic light.

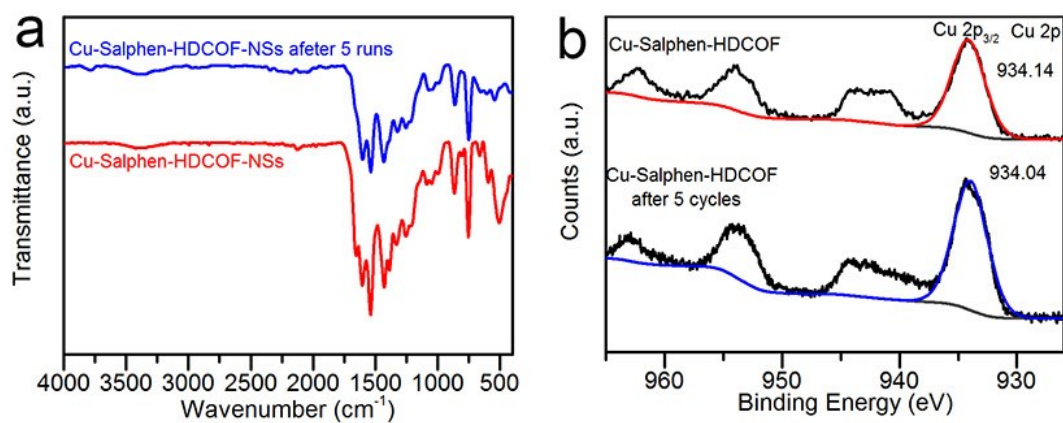


Figure S20. FT-IR and XPS of Cu-Salphen-COF-NSs before (red line) and after 5 runs (blue line) of photocatalytic hydrogen production.

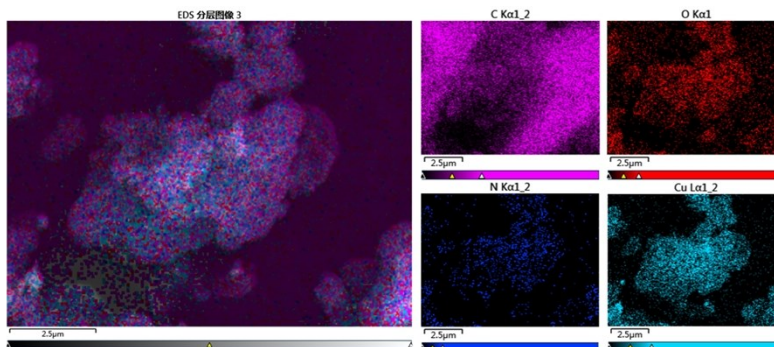


Figure S21. Energy dispersive spectroscopy (EDS) mapping results of the recycled Cu-Salphen-HDCOF-NSs.

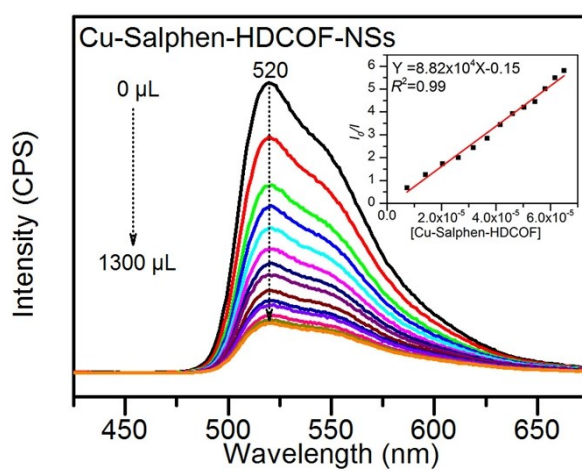


Figure S22. Emission spectra of FS as a function of Cu-Salphen-HDCOF-NSs. Inset: Stern-Volmer plots for the photoluminescence quenching of FS.

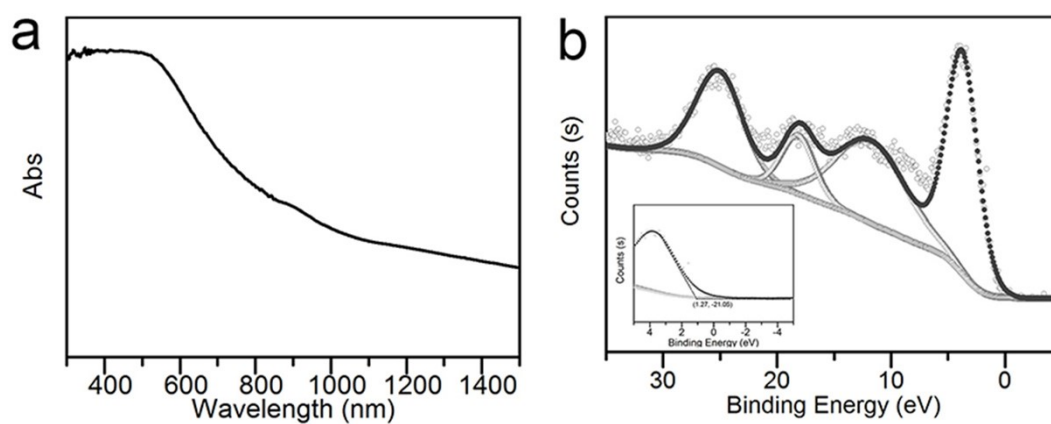


Figure S23. (a) UV-vis diffuse reflectance spectra and (b) VB-XPS spectra of Cu-Salphen-HDCOF.

**Table S1.** EXAFS fitting results.

	Path	N <sup>[a]</sup>	$\Delta E(eV)^{[b]}$	R( $\times 10^2$ ) <sup>[c]</sup>	$\sigma^2(\times 10^3)^{[d]}$	R-factor <sup>[e]</sup>
CuO	Cu-O	4	1.23	0.004	1.943	0.012
CuPc	Cu-Cu	12	7.99(1.17)	354.0(3.49)	6.04(3.65)	0.025
	Cu-N	4	4.92(2.56)	193.5(1.63)	2.66(2.03)	
Cu-Salphen-HDCOF	Cu-N	4.62(0.68)	-4.42(1.90)	194.3(1.20)	4.33(1.58)	0.0146

[a] Coordination number; [b] Inner potential correction; [c] Coordination distance  $\times 100$ ; [d] Debye-Waller factor; [e] The goodness of the fit.

**Table S2.** Elemental analysis of Salphen-HDCOF and Cu-Salphen-HDCOF.

	C (%)	N (%)	H (%)	Cu (%)
Salphen-HDCOF (Calcd.)	77.86	13.35	2.69	---
Salphen-HDCOF	76.51	12.63	1.85	---
Cu-Salphen-HDCOF (Calcd.)	62.87	11.08	1.86	19.60
Cu-Salphen-HDCOF	63.14	12.63	2.76	15.63
Cu-Salphen-HDCOF after 5cycles	64.59	12.06	2.87	14.72

**Table S3.** Photocatalytic H<sub>2</sub>-production performance for catalysts in the literatures.

Photocatalytic systems	Hydrogen Production (mmol g <sup>-1</sup> h <sup>-1</sup> )	Literature
TFPT-COF/Pt/TEOA	1.97	Chem. Sci. <b>2014</b> , 5, 2789 <sup>3</sup>
CdS-COF/Pt/lactic acid	~3.68	Chem. Eur. J. <b>2014</b> , 20, 15961 <sup>4</sup>
N <sub>3</sub> -COF/Pt/TEOA	~1.70	Nat. Commun. <b>2015</b> , 6, 8508 <sup>5</sup>
N <sub>2</sub> -COF/Chloro(pyridine)cobaloxime/TEOA	0.78	J. Am. Chem. Soc. <b>2017</b> , 139, 16228 <sup>6</sup>
PTP-COF/Pt/TEOA	0.083	Faraday Discuss. <b>2017</b> , 201, 247 <sup>7</sup>
FS-COF+WS5F/Pt/ascorbic acid	~16.3	Nat. Chem. <b>2018</b> , 10, 1180 <sup>8</sup>
TP-BDDA-COF/Pt/TEOA	0.3	J. Am. Chem. Soc. <b>2018</b> , 140, 1423 <sup>9</sup>
NH <sub>2</sub> -UiO-66/TpPa-1-COF/Pt/Sodium ascorbate	23.41	Angew. Chem. Int. Ed. <b>2018</b> , 57, 12106 <sup>10</sup>
A-TEPPY-COF/Pt/TEOA	0.006	Adv. Energy Mater. <b>2018</b> , 8, 1703278 <sup>11</sup>
A-TENPY-COF/Pt/TEOA	0.022	Adv. Energy Mater. <b>2018</b> , 8, 1703278 <sup>11</sup>
A-TEBPY-COF/Pt/TEOA	0.098	Adv. Energy Mater. <b>2018</b> , 8, 1703278 <sup>11</sup>
Ru(bpy) <sub>3</sub> Cl <sub>2</sub> /Mo <sub>3</sub> S <sub>13</sub> @EB-COF/Pt/ascorbic acid	13.215	Chem. Commun. <b>2018</b> , 54, 13563 <sup>12</sup>
TpDTz/NiME/TEOA	0.941	J. Am. Chem. Soc. <b>2019</b> , 141, 11082 <sup>13</sup>
sp <sup>2</sup> c-COF/Pt/TEOA	1.36	Chem. <b>2019</b> , 5, 1632 <sup>14</sup>
sp <sup>2</sup> c-COFERDN/Pt/TEOA	2.12	Chem. <b>2019</b> , 5, 1632-1647 <sup>14</sup>
sp <sup>2</sup> c-CMP/Pt/TEOA	0.14	Chem. <b>2019</b> , 5, 1632-1647 <sup>14</sup>
CTF-BT/Th/Pt/TEOA	6.6	Angew. Chem. Int. Ed. <b>2019</b> , 58, 8676 <sup>15</sup>
CTF-BT/Pt/TEOA	1.8	Angew. Chem. Int. Ed. <b>2019</b> , 58, 8676 <sup>15</sup>
CTF-Th/Pt/TEOA	1.1	Angew. Chem. Int. Ed. <b>2019</b> , 58, 8676 <sup>15</sup>
Pt-PVP-BT-COF/Pt/ascorbic acid	0.076	Angew. Chem. Int. Ed. <b>2019</b> , 58, 18290 <sup>16</sup>
Pt-PVP-TP-COF/Pt/ascorbic acid	8.42	Angew. Chem. Int. Ed. <b>2019</b> , 58, 18290 <sup>16</sup>
ter-CTF-0.7/Pt/TEOA	19.3	ACS Catal. <b>2019</b> , 9, 9438 <sup>17</sup>
CN(g-C <sub>3</sub> N <sub>4</sub> )-COF/Pt/TEOA	10.1	Chem. Commun. <b>2019</b> , 55, 5829 <sup>18</sup>
TpPa-COF-(CH <sub>3</sub> ) <sub>2</sub> /Pt/ascorbate	8.33	Chemcatchem <b>2019</b> , 11, 2313 <sup>19</sup>
TpPa-COF/Pt/ascorbate	1.56	Chemcatchem <b>2019</b> , 11, 2313 <sup>19</sup>
TpPa-COF-NO <sub>2</sub> /Pt/ascorbate	0.22	Chemcatchem <b>2019</b> , 11, 2313 <sup>19</sup>
CTF-HUST-A1/NiP <sub>x</sub> /Pt/TEOA	25.4	Angew. Chem. Int. Ed. <b>2020</b> , 59, 6007 <sup>20</sup>
COF-alkene/Pt/TEOA	2.33	Adv. Sci. <b>2020</b> , 7, 1902988 <sup>21</sup>
<b>FS/Cu-Salphen-HDCOF-NS/TEA</b>	<b>36.99</b>	<b>Our Work</b>

## References

- [1] L. Chen, J. Kim, T. Ishizuka, Y. Honsho, A. Saeki, S. Seki, H. Ihee, D. Jiang, *J. Am. Chem. Soc.* 2009, 131, 7287.
- [2] Y. Zang, F. Pei, J. Huang, Z. Fu, G. Xu, X. Fang, *Adv. Energy Mater.* 2018, 8, 1802052.
- [3] L. Stegbauer, K. Schwinghammer, B. V. Lotsch, *Chem. Sci.* 2014, 5, 2789.
- [4] J. Thote, H. B. Aiyappa, A. Deshpande, D. Diaz Diaz, S. Kurungot, R. Banerjee, *Chem. Eur. J.* 2014, 20, 15961.
- [5] V. S. Vyas, F. Haase, L. Stegbauer, G. Savasci, F. Podjaski, C. Ochsenfeld, B. V. Lotsch, *Nat. Commun.* 2015, 6, 8508.
- [6] T. Banerjee, F. Haase, G. Savasci, K. Gottschling, C. Ochsenfeld, B. V. Lotsch, *J. Am. Chem. Soc.* 2017, 139, 16228.
- [7] F. Haase, T. Banerjee, G. Savasci, C. Ochsenfeld, B. V. Lotsch, *Faraday Discuss.* 2017, 201, 247.
- [8] X. Wang, L. Chen, S. Y. Chong, M. A. Little, Y. Wu, W.-H. Zhu, R. Clowes, Y. Yan, M. A. Zwijnenburg, R. S. Sprick, A. I. Cooper, *Nat. Chem.* 2018, 10, 1180.
- [9] P. Pachfule, A. Acharjya, J. Roeser, T. Langenhahn, M. Schwarze, R. Schomaecker, A. Thomas, J. Schmidt, *J. Am. Chem. Soc.* 2018, 140, 1423.
- [10] F.-M. Zhang, J.-L. Sheng, Z.-D. Yang, X.-J. Sun, H.-L. Tang, M. Lu, H. Dong, F.-C. Shen, J. Liu, Y.-Q. Lan, *Angew. Chem. Int. Ed.* 2018, 57, 12106.
- [11] L. Stegbauer, S. Zech, G. Savasci, T. Banerjee, F. Podjaski, K. Schwinghammer, C. Ochsenfeld, B. V. Lotsch, *Adv. Energy Mater.* 2018, 8, 1703278.
- [12] Y.-J. Cheng, R. Wang, S. Wang, X.-J. Xi, L.-F. Ma, S.-Q. Zang, *Chem. Commun.* 2018, 54, 13563.
- [13] B. P. Biswal, H. A. Vignolo-Gonzalez, T. Banerjee, L. Grunenberg, G. Savasci, K. Gottschling, J. Nuss, C. Ochsenfeld, B. V. Lotsch, *J. Am. Chem. Soc.* 2019, 141, 11082.
- [14] E. Jin, Z. Lan, Q. Jiang, K. Geng, G. Li, X. Wang, D. Jiang, *Chem* 2019, 5, 1632.
- [15] W. Huang, Q. He, Y. Hu, Y. Li, *Angew. Chem. Int. Ed.* 2019, 58, 8676.
- [16] J. Ming, A. Liu, J. Zhao, P. Zhang, H. Huang, H. Lin, Z. Xu, X. Zhang, X. Wang, J. Hofkens, M. B. J. Roeffaers, J. Long, *Angew. Chem. Int. Ed.* 2019, 58, 18290.
- [17] L. Guo, Y. Niu, S. Razzaque, B. Tan, S. Jin, *ACS Catal.* 2019, 9, 9438.
- [18] M. Luo, Q. Yang, K. Liu, H. Cao, H. Yan, *Chem. Commun.* 2019, 55, 5829.
- [19] J.-L. Sheng, H. Dong, X.-B. Meng, H.-L. Tang, Y.-H. Yao, D.-Q. Liu, L.-L. Bai, F.-M. Zhang, J.-Z. Wei, X.-J. Sun, *Chemcatchem* 2019, 11, 2313.
- [20] S. Zhang, G. Cheng, L. Guo, N. Wang, B. Tan, S. Jin, *Angew. Chem. Int. Ed.* 2020, 59, 6007.
- [21] C. Mo, M. Yang, F. Sun, J. Jian, L. Zhong, Z. Fang, J. Feng, D. Yu, *Adv. Sci.* 2020, 7, 1902988.